N72-29332

SECTION 32

CLASSIFICATION OF SPATIALLY UNRESOLVED OBJECTS*

by

Richard F. Nalepka
Harold M. Horwitz
Peter D. Hyde
James P. Morgenstern
Willow Run Laboratories
University of Michigan
Ann Arbor, Michigan

The practical utility of multispectral scanner data is often restricted by the limited spatial resolution of the sensor gathering the data. Restrictions of this sort will exist in the data to be gathered by the multispectral scanners in the ERTS-A and SKYLAB satellites. These scanners will view the ground with an instantaneous field of view (IFOV) covering a ground patch about 300 feet on a side. The radiation detected when scanning portions of a scene containing objects smaller than this size will be composed of a mixture of radiation from all objects within the IFOV. Similarly, when the field of view overlaps the boundary between two larger objects, the radiation detected will be a mixture from the two objects. The signals generated by the sensor in both of these cases will not be representative of any one object.

The effect of viewing more than a single object class is illustrated in Figures 1 and 2. In Figure 1 the reflectance spectra are depicted for corn and bare soil as they would appear individually. If the sensor was to simultaneously view both corn and bare soil the effective reflectance spectrum would be quite different. This is shown in Figure 2 for the combinations 20% corn - 80% bare soil and 50% corn - 50% bare soil. These spectra are simply weighted combinations of the pure spectra of Figure 1.

The use of standard multispectral recognition processing techniques on data points which result from viewing two or more objects will likely result in the improper classification of those data points. Given a

* The work reported in this paper was supported by NASA under Contract NAS9-9784.

sufficient number of improper classifications of this sort the results of such efforts as might be applied in crop acreage determination, for example, would be greatly in error.

It might be useful, at this point, to provide some idea of the seriousness of this effect. Figure 3 illustrates the effect of sampling and reconstructing a scene using a sensor whose resolution is approximately the size of the structure in the scene. For illustrative purposes the scene is composed of black and white squares arranged as on a checkerboard. Obviously if the resolution of the sensor was significantly smaller than the dimensions of the square, the scene could be reconstructed with very good fidelity. However, this will generally not be the case for either the ERTS or SKYLAB multispectral sensors.

In Figure 3 we consider two situations. One in which the resolution is one half that of the squares and another in which the resolution exactly equals the square size. Now, it is possible for both these situations to perfectly reconstruct the scene. The probability of this occurring, however, is very slim since the samples must be taken only at those times during which the sensor is viewing portions of all of either the black or the white square. It is much more likely that in an attempt to sample the entire scene, that is leave no voids between samples in either direction, many samples would be extracted when the sensor was viewing some portion of each of two or more adjacent squares. In this case the scene could not accurately be reconstructed.

In the lower portion of Figure 3, we depict the reconstruction of the scene for the resolution being one half the square size (lower left) and equal to the square size (lower right). Here we consider the worst situation that may exist since we can have no assurance beforehand that this will not in fact be the case for an arbitrary scene for which the sampling scheme has not been specifically designed. For the resolution of one half the square size, the samples which fall totally within each square fall precisely in the center of the squares. All other samples, therefore, are extracted when half the sensor field of view covers white squares and the other half covers black squares. The sensor signals generated in this situation are not characteristic of either of the objects in the scene. In this case the use of standard automatic processing techniques for classification and determination of the ground area covered by each of the two objects in the scene, would result in significant errors. In this particular case 50% of the scene area would be improperly classified. For the situation where the resolution equaled the square size the error would be 100% since not a single sample would be classified correctly.

We have carried out some calculations to get a feeling for how serious this problem may be for spaceborne sensors viewing an instantaneous ground patch 300 feet on a side. The results of the calculations are plotted in Figure 4 which illustrates the effect of field area and shape on the multispectral training and classification operations. Just as before we consider fields which are square in shape, however in addition, we also consider rectangular fields. The dimensions of both square and rectangular fields are integral multiples of 300 feet and all sampled areas which occur at field boundaries are assumed to fall one half (at the corners this is three quarters) outside the field. For the rectangular fields the small dimension is limited to 600 feet. Square fields and rectangular fields of this sort define the limiting conditions (best and worst) for regularly shaped areas.

Two pairs of curves are plotted in Figure 4. The curves depicted as dashed lines relate the number of acres in a field to the number of 300 by 300 foot elements totally within the field. This relationship is significant when considering the requirements for training a recognition computer. The number of samples generally considered necessary for an adequate determination of the statistics defining a multispectral signature is ten times the number of spectral channels being utilized. If the four ERTS channels were considered, a minimum of 40 representative samples would be required. To assure this number of samples in a single field would require a square field of at least 110 acres and a 2 x n element rectangular field of 170 acres or so.

If, however, training of the computer had already been accomplished, it would be desirable to know what errors might be expected in automatically determining the area covered by a selected set of object classes. This information is also plotted in Figure 4. The curves depicted as solid lines relate the number of 300 by 300 foot elements in the field to the percentage of the field area which is seen in combination with portions of adjoining fields. It is this area which would probably be classified incorrectly and produce the errors in area computed. For the 110 acre square field described before, 40 elements were totally within the field and a 25% error in the determination of the area of that field could be expected. A 51% error in the area of the 170 acre rectangular field could be expected.

Not only are these errors of significant size, but if one is considering carrying out agricultural surveys, the field sizes considered above are somewhat larger than is typical in many agricultural areas. As shown in Figure 4 larger errors would result for smaller fields.

In order to reduce the restrictions on the utility of remotely sensed multispectral data, personnel of the Willow Run Laboratories have been conducting theoretical studies to develop special processing and information extraction techniques which will enable the accurate and timely estimation of the proportions of objects and materials appearing within the IFOV of a remote multispectral sensing device.

It is the fact that the radiation emanating from each scene element is detected simultaneously in several spectral bands which offers the possibility for classifying and estimating the proportions of spatially unresolved objects. The model that we have used to describe the signature generated in viewing a mixture of objects is as follows:

$$A_X = \sum_i X_i A_i$$

$$M_X = \sum_i X_i M_i$$

where the signature of Type i material is a Gaussian distribution with mean A_i and covariance matrix M_i and the proportion of Type i material is X_i.

As long as the radiation spectra generated by objects within the IFOV are linearly independent, i.e., a unique radiation spectrum results for each combination of objects, a satisfactory solution will usually be possible. This requirement is somewhat more limiting than that imposed for standard recognition processing. In Figure 5 we illustrate two separate plots of the means and distribution contours (signatures) of three objects as seen in two spectral bands. In each case the signatures of the three objects are sufficiently separate so that if any one of them was viewed in its pure state it could easily and properly be classified. For the case depicted in the upper portion of the figure, combinations of the three objects would produce points generally falling within the triangle and using the specially developed techniques the proportions of these objects could be determined. The lower portion of the figure, however, depicts a situation where the pure signature for object A_1 exhibits characteristics very similar to a combination of the other two objects. In this case the proportions of a mixture of these objects could not be accurately determined. Although all possible sets of objects and materials of interest may not meet the requirements for linear independence, it is believed that the requirements are met often enough to make the solutions now being investigated potentially very useful.

During the last year our primary efforts have been directed towards searching for computational algorithms which could both efficiently and accurately estimate the proportions of mixtures of objects. Three potentially useful algorithms were located, implemented via digital

computer programs, and tested. In order to provide the control necessary for the proper testing of these algorithms all tests were carried out using artificially generated mixtures. In some cases the pure signatures used to generate the artificial mixtures were extracted from data gathered by The University of Michigan multispectral scanner while in other situations totally artificial signature sets were constructed.

The latter was the case when tests were run to compare the processing time of the three computational methods as a function of the number of signatures employed. Here the pure signatures were arranged to form a symmetric set exhibiting identity covariance matrices and separated from each other by a unit distance. Two sets of 100 data points were generated. One set was distributed normally about the centroid of the signatures (the equal proportion situation) while the other set was similarly distributed about one of the signature means.

In Figure 6 we see that the computation time is a function of the location of the data points with respect to the pure signatures for all three methods considered. For two of the three methods (the F and the C methods) the computation time required for data points at or near the centroid exceeds that for points at or near the vertex. The opposite is true for the T method. These differences are a result of differences in the manner in which proportions are estimated in each method.

It is clear that as the number of signatures increases the computation time also increases. The best overall method seems to be the C method. However, for small numbers of signatures and data points near the centroid the T method would do just as well. As illustrated in Figure 6, the computation of proportions for each data point is a relatively time consuming task. The time required is approximately an order of magnitude greater than standard processing and four orders of magnitude greater than data collection. Some reductions in processing time could be achieved by utilizing larger and more up to date computer facilities but still the time required would be significant.

In many applications, proportions for each data point may not be required. For these cases a reduction in computation time can be achieved by averaging many data points and then carrying out a single computation of the proportions of the objects appearing in the entire region which was averaged. This approach is not only much faster but it also provides the possibility for improved accuracy. Improved accuracy might result since averaging would reduce the effect of the variability of sensor signals due to the natural variation of the radiation received from any object class in the scene. In addition, the effects of random noise would be reduced.

In order to test the averaging approach, signatures for bare soil, weeds, alfalfa, and barley were extracted from multispectral scanner data gathered by The University of Michigan. A total of 400 data points were generated with each set of 100 being normally distributed about the mean of artificial mixtures indicated in columns 2-5 of Table I. These 400 data points were averaged and an estimate of the proportions for the single average data point was computed. The results of the computation are given in column 7. Upon comparison with the average of the specified proportions shown in column 6 it is obvious that the estimated proportions are quite accurate, exhibiting a maximum error of 1.5%.

We are now preparing to apply these proportion estimation techniques to real data to identify any unforeseen problems which may arise in operating on real data sets, to refine or modify the approach to overcome these problems, and to provide a more realistic demonstration of the potential of these techniques.

TABLE I. TEST OF AVERAGING APPROACH TO ESTIMATE PROPORTIONS
(Artificial Mixtures)

MATERIAL	SPECIFIED PROPORTIONS 100 PTS.	SPECIFIED PROPORTIONS 100 PTS.	SPECIFIED PROPORTIONS 100 PTS	SPECIFIED PROPORTIONS 100 PTS.	AVE. SPECIFIED PROPORTIONS 400 PTS.	ESTIMATED PROPORTIONS	ERROR
BARE SOIL	0.25	0.35	0.10	0.20	0.225	0.234	0.009
WEEDS	0.25	0.20	0.50	0.35	0.325	0.320	0.005
ALFALFA	0.25	0.15	0.20	0.30	0.225	0.210	0.015
BARLEY	0.25	0.30	0.20	0.15	0.225	0.236	0.011

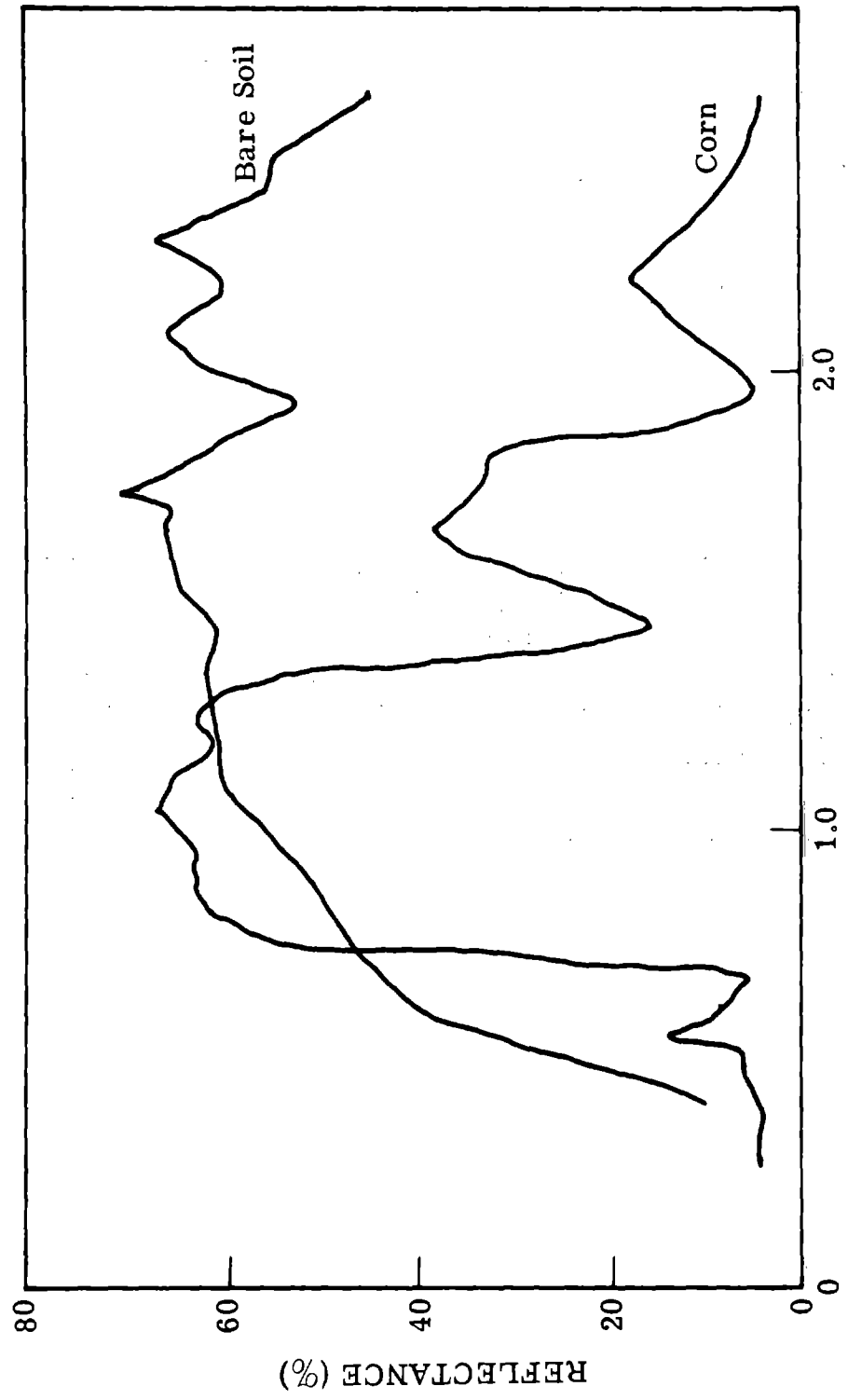

FIGURE 1. REFLECTANCE SPECTRA

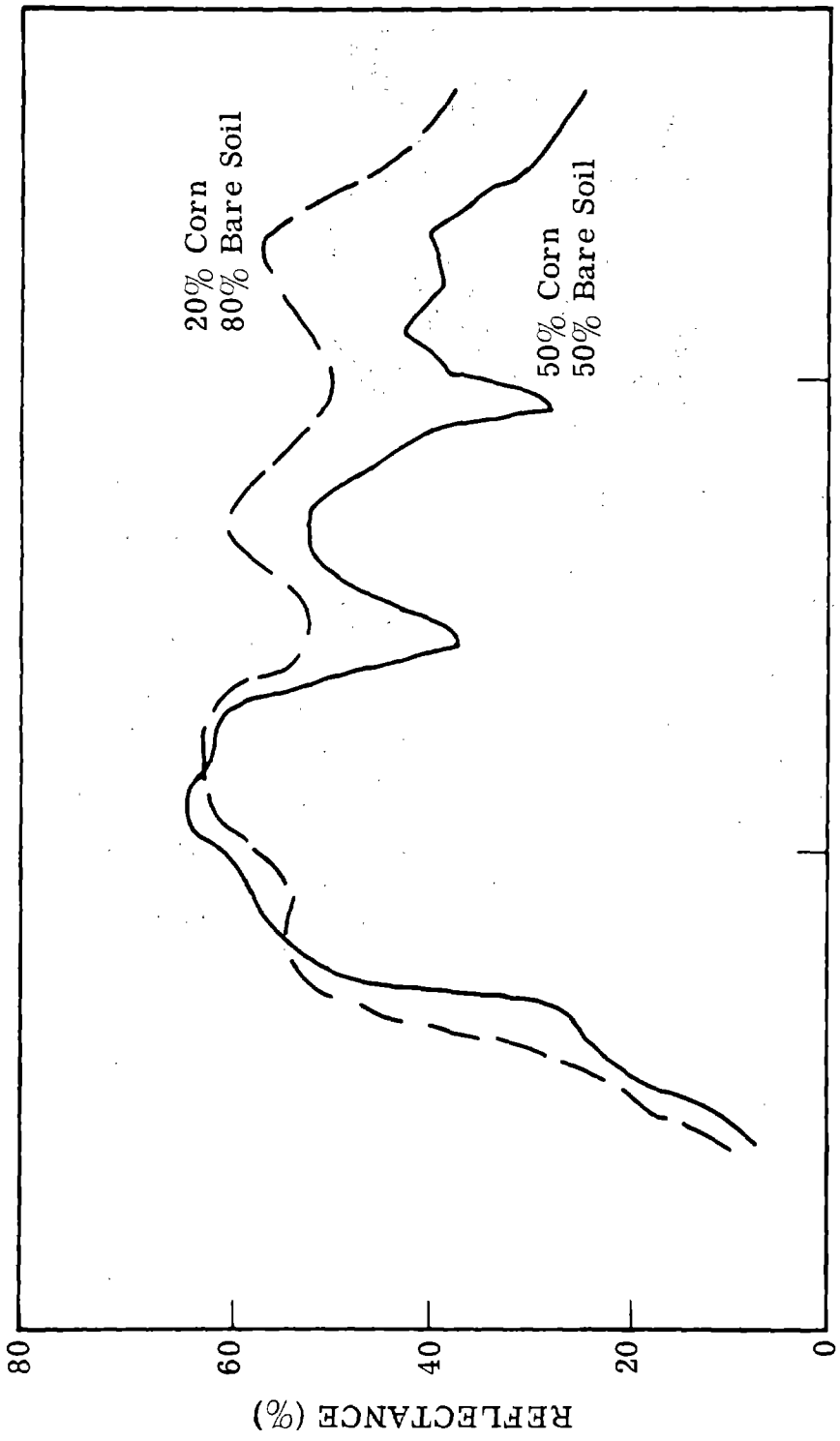

FIGURE 2. REFLECTANCE SPECTRA OF MIXTURES

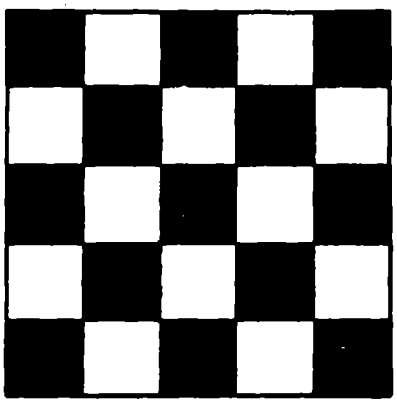

Checkerboard Scene

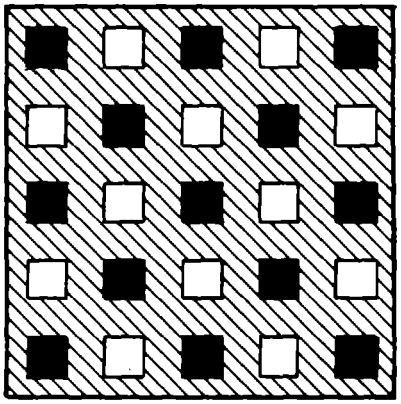

Reconstructed Scene
Optical Resolution Equals
One Half Checkerboard
Cell Size (Worst Case)

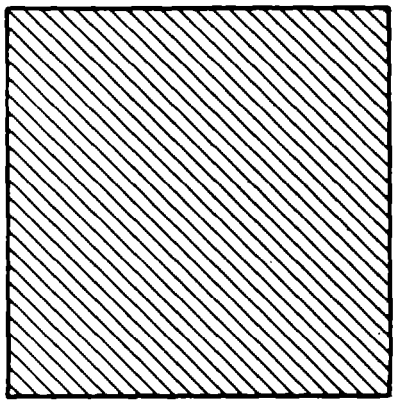

Reconstructed Scene
Optical Resolution Equals
Checkerboard Cell Size
(Worst Case)

FIGURE 3. EFFECT OF SAMPLING AND RECONSTRUCTING A SCENE WITH OPTICAL RESOLUTION APPROACHING THE SCENE STRUCTURE SIZE

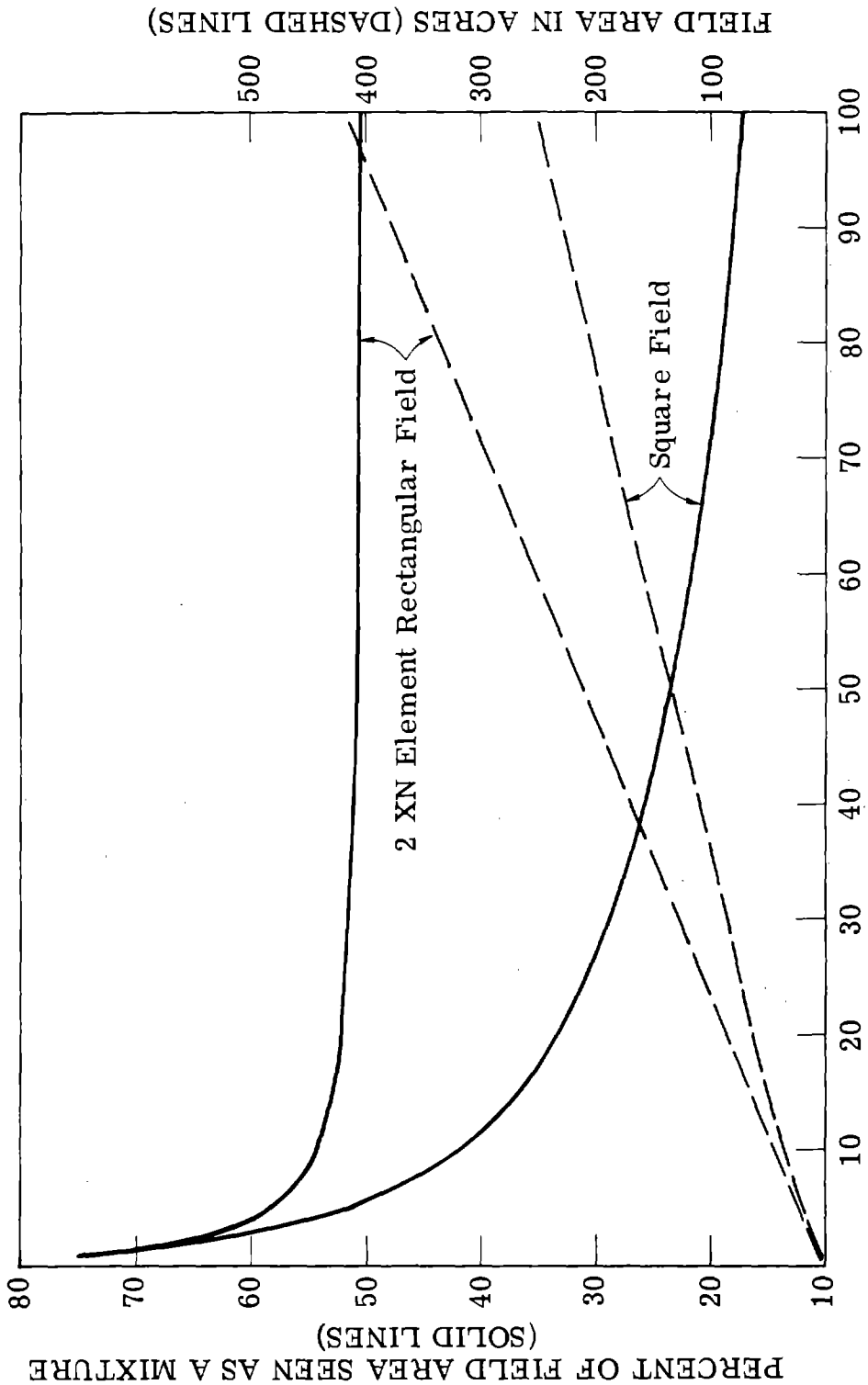

FIGURE 4. THE EFFECT OF FIELD AREA AND SHAPE ON MULTISPECTRAL TRAINING AND CLASSIFICATION FOR 300 X 300 ft. OPTICAL RESOLUTION

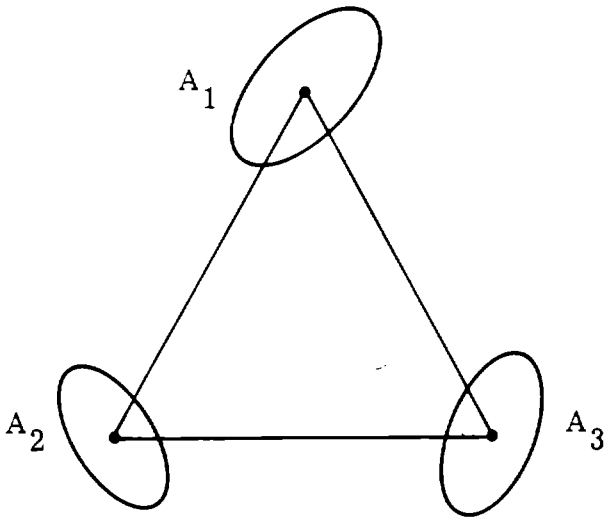

(a) Signature Simplex with Unit Contour Ellipsoids

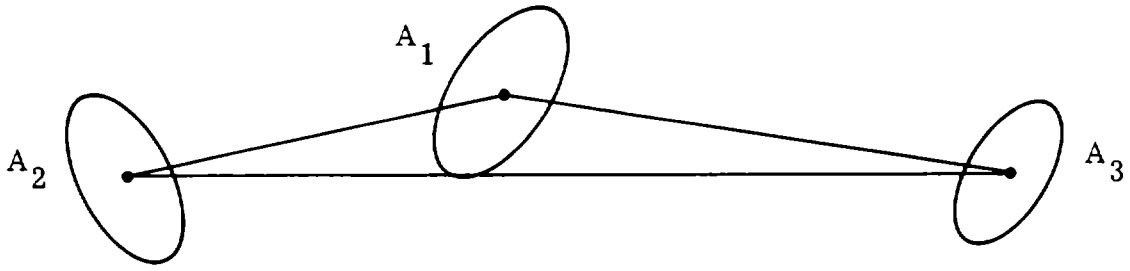

(b) Nearly Degenerate Signature Configuration

FIGURE 5. GEOMETRIC CONFIGURATION FOR THREE SIGNATURES AND TWO CHANNELS

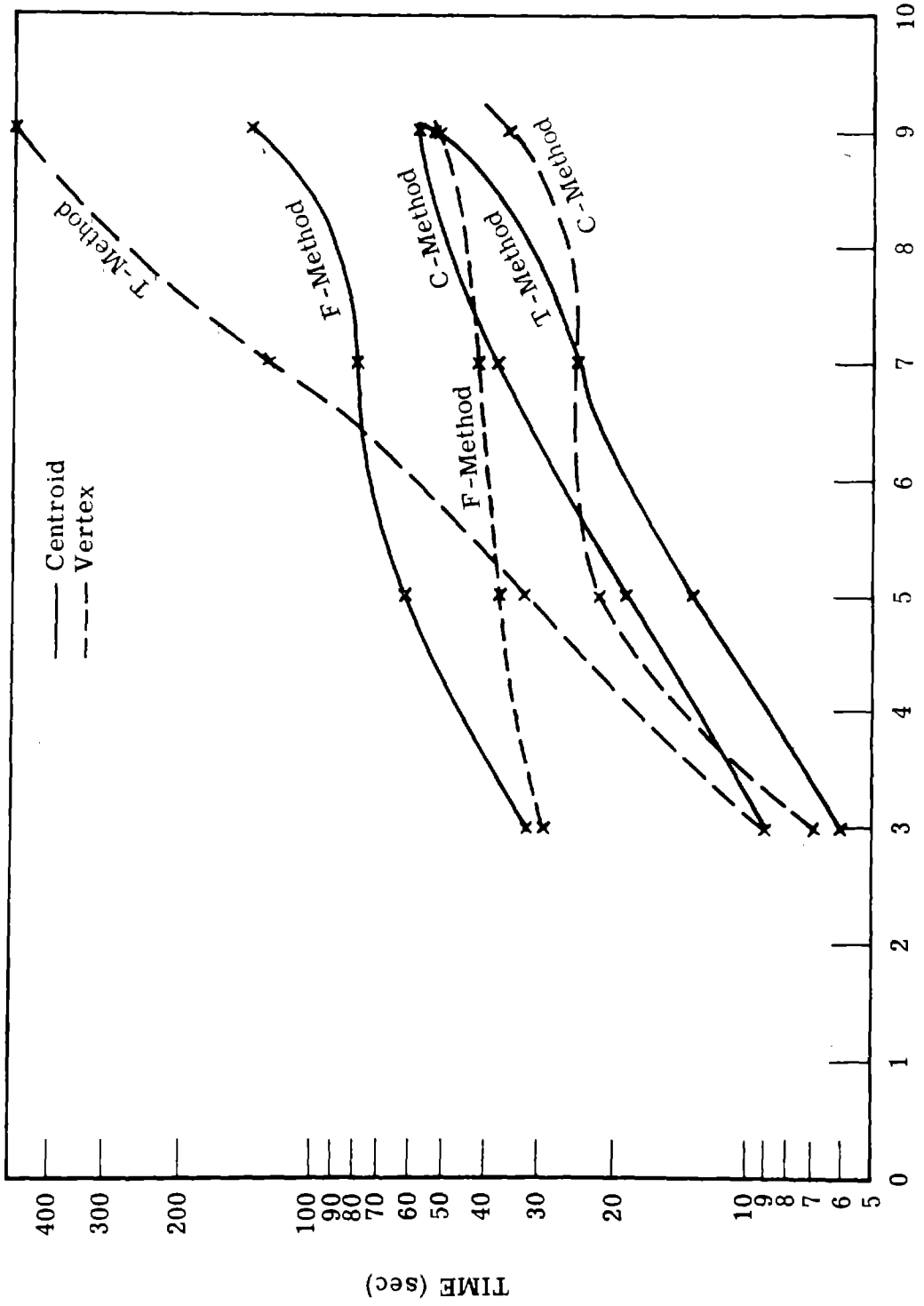

FIGURE 6. PLOTS OF RUNNING TIME VERSUS NUMBER OF SIGNATURES (CENTROID AND VERTEX)